

**RESEARCH**

# Collection and Characterization of Synthetic Airborne Particles

Marian-Catalin Grosu<sup>1,\*</sup>  | Emilia Visileanu<sup>1</sup> | Alexandra Gabriela Ene<sup>1</sup> | Razvan Victor Scarlat<sup>1</sup> | Virgil Emanuel Marinescu<sup>2</sup>

<sup>1</sup>The National Research & Development Institute for Textiles and Leather, 16 Lucretiu Patrascanu, Sector 3, Bucharest, 030508, Romania

<sup>2</sup>The National Institute for Research and Development in Electrical Engineering ICPE-CA Bucharest (ICPE-CA), 313 Splaiul Unirii, Sector 3, Bucharest, 030138, Romania

**Corresponding author**

E-mail: [catalin.grosu@incdtp.ro](mailto:catalin.grosu@incdtp.ro)  
Tel.: +40213404928

**Web of Science Researcher ID:**

Marian Catalin Grosu  
GLQ-6850-2022

**ABSTRACT**

This paper presents the polypropylene (PP) micro-nano particles (MNPs) exposure routes of textile industry personnel and analyses the characteristics of such particles collected in and outside the workplaces. A Laser Aerosol Spectrometer set was used to determine: the total suspended particles (TSP), PM10, PM2.5, PM1 fractions ( $\mu\text{m}/\text{m}^3$ ), and the total number of particles (TC) (1/l) from the air. Specific methods for descriptive statistics were used to characterize the particle populations. Mean, dispersion and standard deviation, median and quartiles, skewness and kurtosis for asymmetry, and highlighting the cases in which they should be performed were calculated. The Box plot box-plots and histograms graphs for TSP, PM10, PM2.5, and PM1, TC variables. The comparative analysis of the results led to the identification of the fraction of the particles with the highest value concentration in the air. The particles were collected on quartz and polycarbonate filters with gold membrane using TECORA and GilAirPlus pumps. The mass of particles collected was determined by weighing the filters before and after collection, using an electronic balance. Characterization of PP dust collected by analysis: Optical microscope, Scanning Electron Microscopy,  $\mu$ Raman spectroscopy, FTIR, and TG-DSC allowed the identification of the shape, size, and structural footprint of PP particles.

**KEYWORDS**

Polypropylene MNPs, SEM, FTIR, TG-DSC.

**INTRODUCTION**

As part of anthropogenic particles (APs), micro and nano plastic (MNPs) particles and fibers represent a global scale contamination source with hazard potential [1]. In the nanotechnology field, “nano plastic” may refer to engineered particles <100 nm, i.e., the nanotechnology application size limit, while “microplastic” is often known as particles up to 5 mm in dimensions with no defined lower size limit [2].

Increases in plastic-related pollution and their weathering can be a serious threat to environmental sustainability [3]. According to United Nations Environment Program (UNEP), plastic contamination and associated weathering mechanisms are emergent environmental and human health and human food chain concerns [4]. There, primary microplastic is either

produced as microparticles or enters the natural environment already as microparticles. Whereas secondary microplastic is generated by fragmentation or abrasion of other products in the natural environment. Both pollute the global ecospheres and even enter the human food chain. Also, plastic cups and bottles used for mineral water packaging may release plastic particles during continuous exposure to heat, light, or unfavorable chemical environments during transportation and storage. The concentration of the plastic particles released in such cups and bottles rapidly increase under irradiation as a function of exposure time [5].

Now, MNPs are omnipresent in our environment (e.g., biota/gut content, water, sediment, and foodstuffs) [6].

Thought to be the most important sources of primary microplastics can mention: the production, use, and recycling of synthetic textiles, including plastic fragments

This is an open access article licensed under the Creative Commons Attribution 4.0 International License, which allows for use, distribution, and reproduction in any medium as long as the original work is properly cited. © 2023 The Authors. The International Association of Advanced Materials, Sweden, publishes Advanced Materials Letters.

from clothes and house furniture, erosion of synthetic rubber tires, and particles released from traffic, city dust, materials in buildings, waste incineration, landfills, industrial emissions, particle resuspension, synthetic particles used in horticultural soils (e.g. polystyrene peat), sewage sludge used as fertilizer and possibly tumble dryer exhaust. The wind transfer is estimated to be responsible for 7% of ocean contamination [7].

Gossmann et al. show that evaluating the potential of spiderwebs as an easily accessible and cheap natural approach to mirror MP air contamination on a spatial and temporal scale. Due to the ubiquitous appearance of spiders and the sticky nature of spider webs, they provide ideal conditions to trap particles, fibers, and fragments, which has already been proven for inorganic compounds [8].

Several in vitro studies on human cells and in-vivo studies on animals show that when tiny plastic particles enter the body through the food chain or respiratory tract, these may accumulate there over time and may cause a variety of serious biological conditions, including oxidative stress, cytokine secretion, cell damage, inflammation or immune reactions, DNA damage, metabolic effects, and neurotoxicity [9-11].

Moreover, the surface charge of microparticles can affect their toxicity. A typical property to quantify the surface charge of microparticles is the particles'  $\zeta$ -potential which can be a proxy for the electrostatic interactions of microparticles with cells and tissues, determining the adhesion of the microparticles. The adhesion strength of microparticles could potentially affect their bioavailability and consequently the toxicity of these particles. More, adverse health effects such as pneumoconiosis, chronic bronchitis, lung and bowel cancer, etc are reported [5].

The textile industry, as a major polluter worldwide, generates micro and nano plastic particles during the manufacturing processes, especially nylon, polyester, polyurethane, polyolefin, acrylic, and vinyl-type polymers. Various reviews highlight synthetic textiles as the main superordinate source of airborne microplastics and fibers were the most abundant shape of MP found in the atmosphere [12,13].

An important source of particle pollution is the emissions from the preparation of spinning, (opening, blending, lap forming, carding, combing, etc.), and the manufacture of fabrics, knits, and non-wovens that form a suspension, which over time settle on every surface. Dust, fragments of fibers, and also lint is produced by processing natural and synthetic staple fibers before and during spinning as well as in the following processing steps. [14]

A cross-sectional study carried out by Paudyal *et al.*, (2010) in four different textile sectors (garments, carpet production units, weavers and recycling units) in Nepal shows that almost 18% of the workers included in the sample, breathe air with exceeded limits of impurities at the workplace [15].

Another 2013 research reinforces the idea that exposure to particulate matter in the atmosphere is

dangerous for textile workers. So, Sangeetha et al. carried out an analysis of the amount of PM 2.5 and PM10 particles in different textile knitting and garment departments by collecting indoor air samples. The study also presents permissible exposure limits (PELs) for airborne particles resulting from cotton processing in different work areas. These limits can vary between 200  $\mu\text{g}/\text{m}^3$  and 750  $\mu\text{g}/\text{m}^3$  depending on the production sector/workplace [16].

Polypropylene (PP) is regarded as one of the lightest and most versatile semi-crystalline thermoplastic polymers, capable of undergoing a wide array of manufacturing processes including textile and non-textile fields. commercial PP is typically a mixture of 75% isotactic and 25% atactic. While the demand for PP is rapidly on the increase and consequently, it is one of the most common types of microplastic found in every environment [17].

In this paper, polypropylene micro and nanoparticles, generated during technological textile processes are counted and collected to characterize them. This is the first part of the research, that will continue with the toxicological toxicity tests, which will be performed after collecting biological samples (blood, saliva, nose swap) from the workers.

The technological process of manufacturing narrow articles for straps, belts, etc. with domestic and industrial uses has been selected due to the friction phenomenon to which PP yarns are subjected during processing the most determined large quantities of particles released into the air. The determination was made at a Romanian textile company that processes polypropylene yarns, encoded HT.

## EXPERIMENTAL

### *Textile processing workplace*

The chosen sampling workplace is a textile weaving mill that processes PP filamentary yarns 1112,0x1dtex (1000, 8x1 den), using Jacob Muller looms to produce narrow woven fabrics and ribbons and trimmings.

### *Procedure and equipment for determining the concentrations/number of particles in the air*

The online procedure for determining the total (TSP) and fractions PM10, PM2.5, and PM1 concentrations ( $\mu\text{g}/\text{m}^3$ ) and the total number of particles (TC), respectively were applied. For determinations, a portable Grimm LASER AEROSOL SPECTROMETER MINI LAS model 11-E was used. The mini device uses high-tech laser optics to capture each particle with dimensions between 0.25 and 32  $\mu\text{m}$  and classifies them into 31 size channels (via software: according to the European standard EN 481).

The results of the determinations of the concentrations of the particles released during the technological process (in the proximity of the workplaces (narrow weaving looms) and outside are presented comparatively in the section on results and discussions.

**Equipment and procedure for the sampling of particles**

The collection, to identify some parameters of shape and structure of the particles identified at HT, was done using 2 types of devices, using different filters both in terms of constituent raw material (quartz, nucleopore type polycarbonate with gold coated membrane). It was necessary to use filters of different natures and sizes, due to the technological limitations of the equipment for analysis and characterization of the content deposited on them (micro and nanoparticles, respectively microfibers). The equipment used for particles/fibers collection is presented in **Table 1**, which contains also, information on the filters, and main parameters used.

The collection of particles/fibers was made from the proximity of 3 narrow weaving looms (encoded M1, M2, and M3), on filters F1AM1 (quartz filter,  $\phi$  47 mm - Tecora - machine 1), F2BM2 (quartz filter,  $\phi$  37mm - GilAirPlus - machine 2) and F3BM3 (gold coated polycarbonate filter,  $\phi$  25 mm - GilAirPlus - machine 3). The collection in the proximity of each weaving loom was repeated 3 times, in the same working conditions. The quartz filters were pre-treated by calcinating at a temperature of 600°C – 800°C for 6 hours. Each filter was weighed before and after collection, using A&D BM 20 analytical scale.

**Table 1.** Sampling devices and parameters.

o.	Air sampling device	Air sampling parameters
A.	<b>Tecora Skypost PM-FG</b> - Skypost PM-HV pump, impactors, electronic flow rate control (< 50 l/min); Standard: EN12341:2014	Filter F1: $\phi$ 47 mm quartz fiber membrane, porosity: 0.4 microns; Airflow: 38 l/min
B.	<b>GilAirPlus</b> – unplugged, device, equipped with QuadMode <sup>SM</sup> air sampling technology, constant flow (0.01 - 5 l/min); Standard: EN 1232	Filter F2: $\phi$ 37 mm quartz fiber membrane; Filter F3: $\phi$ 25 mm, polycarbonate gold coated membrane, porosity: 0.2 microns; Airflow: 2l/min

**RESULTS AND DISCUSSION**

**Fig. 1(a,c,e,g,i)** shows the histograms and **Fig. 1(b,d,f,h,j)** the box plots, made with the specialized software, corresponding to the results of the determinations of total (TSP) and fractions of the suspended particles PM10, PM2.5, PM1 ( $\mu\text{g}/\text{m}^3$ ), respectively the total number of particles TC (1/l).

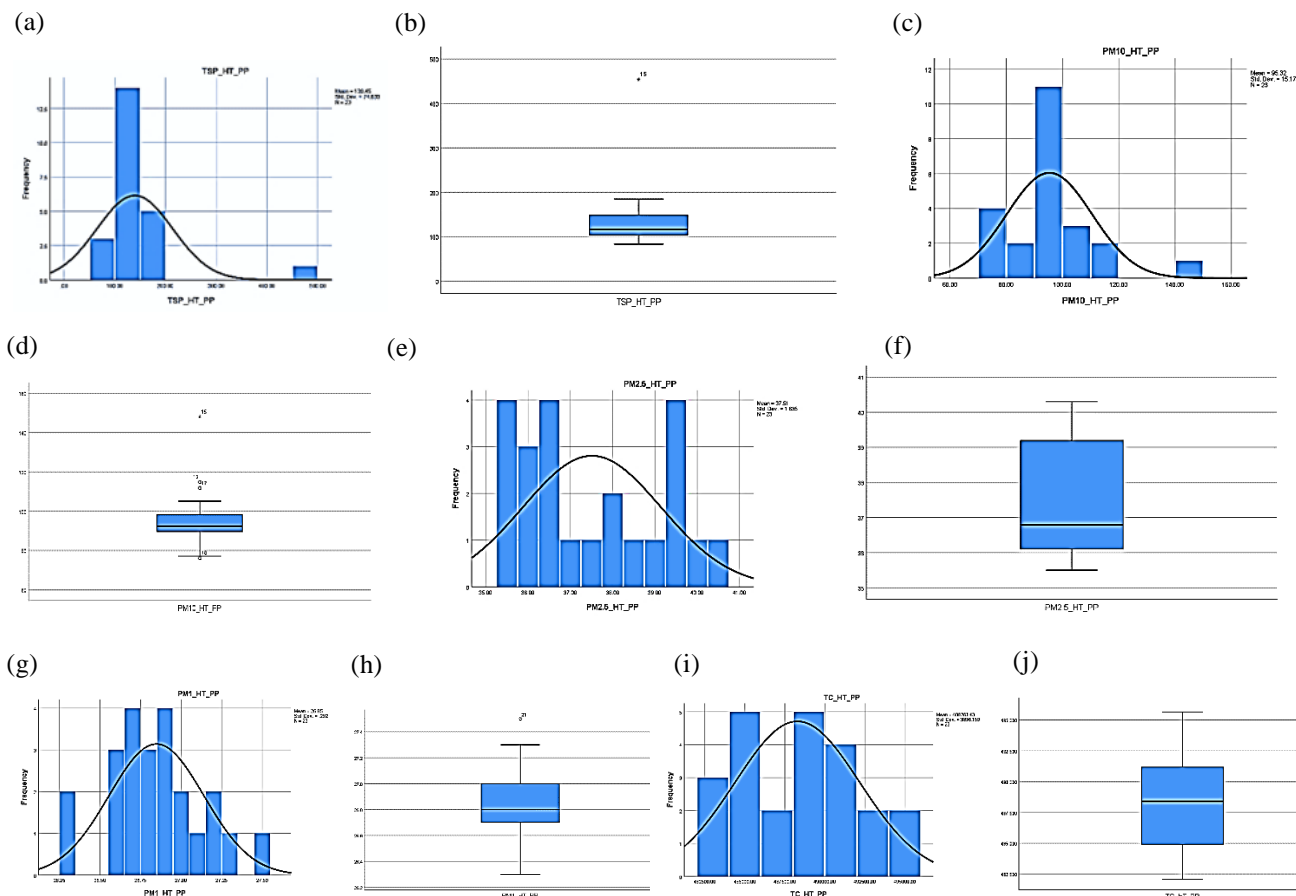


**Fig. 1.** Histograms and boxplots for (a) and (b) TPS, (c) and (d) PM10, (e) and (f) PM2.5, (g) and (h) PM1, (i) and (j) TC.

The analysis of the presented data shows the following aspects:

**Variability**

- The variable TSP (**Fig. 1b**) presents a value with the indicative 15, respectively a registered value of 454  $\mu\text{g}/\text{cm}^3$ . The variable shows the distribution of 50% of the values directed to the left, the median being directed towards the top of the box, so the small values are predominant;
- The variable PM10 (**Fig. 1d**) has values with the indicative: 10 with a value of 76.1  $\mu\text{g}/\text{cm}^3$  and 12 with a value of 114.8  $\mu\text{g}/\text{cm}^3$ , 17 with a value of 111.8  $\mu\text{g}/\text{cm}^3$  which are located in the range 1.5 - 3 box lengths and a value with indicative 15 with the value of 148.1 which is located outside the mentioned range. The variable shows the distribution of 50% of the values directed to the left, the median being directed towards the bottom of the box, so the small values are predominant;
- The variable PM2.5 (**Fig. 1f**) shows values located inside the box. The variable shows the distribution of 50% of the values directed to the left, the median being directed towards the bottom of the box, so the small values are predominant;
- The variable PM1 (**Fig. 1h**) presents values the indicative: 21 with a value of 27.5  $\mu\text{g}/\text{m}^3$  which is in the range of 1.5 3 box lengths. The variable shows the distribution of 50% of the values directed to the left, the median being directed towards the top of the box, so the small values are predominant;
- The variable TC (**Fig. 1j**) does not show values located outside the box. The variable shows the distribution of 50% of the values directed to the right, the median being directed towards the top of the box, so the large values are predominant.

**Distribution form indicators for the analyzed variants:**

- TSP: 25% of the values are below 103.37  $\mu\text{g}/\text{cm}^3$ , 50% are in the range 116.3 -153.47  $\mu\text{g}/\text{cm}^3$  and 25% over 153.47  $\mu\text{g}/\text{cm}^3$ ;
- PM10: 25% of the values are below the value of 89.47  $\mu\text{g}/\text{cm}^3$ , 50% are in the range of 92.43 - 99.20  $\mu\text{g}/\text{cm}^3$  and 25% over 99.20  $\mu\text{g}/\text{cm}^3$ ;
- PM2.5: 25% of the values are below 36.05  $\mu\text{g}/\text{cm}^3$ , 50% in the range 36.8-39.15  $\mu\text{g}/\text{cm}^3$  and 25% above 39.15  $\mu\text{g}/\text{cm}^3$ ;
- PM1: 25% of the values are below the value of 26.8  $\mu\text{g}/\text{cm}^3$ , 50% within the limits of 26.82-27.01  $\mu\text{g}/\text{cm}^3$  and 25% over 27.01  $\mu\text{g}/\text{cm}^3$ ;
- TC: 25% of the values are below 484755.7/l, 50% in the range 488400/l - 491277/l, and 25% above 491277 l.

The asymmetry indices (*skewness*) have the values: of 3.6 for TSP, 1.9 for PM10, 0.336 for PM2.5, 0.186 for PM1, and 0.120 for TC, which highlights the extent to which the mean deviates from the median and implicitly the curves

The normal distribution moves away from the middle, moving to the right.

The vault indices (*kurtosis*) have positive values for the variables TSP (**Fig. 1a**), PM10 (**Fig. 1c**), and PM 1 (**Fig. 1g**), the curves being of leptokurtic type, and have a negative value for the variables PM 2.5 (**Fig. 1e**) and TC (**Fig. 1i**), the curves being of platykurtic type.

Comparing the values for the variables TSP, PM10, PM2.5, PM1, and TC obtained in the vicinity of the workplaces with those obtained outside, a decreasing tendency of the latter can be observed.

The results of the collections on the 3 filters F1AM1, F2BM2, and F3BM3 are presented graphically in **Fig. 2**. The calculations used the average values for the mass of collected particles ( $\mu\text{g}$ ) (**Fig. 2a**), the concentration of particles in the air ( $\mu\text{g}/\text{m}^3$ ) (**Fig. 2b**), respectively the volume of air (l) (**Fig. 2c**).

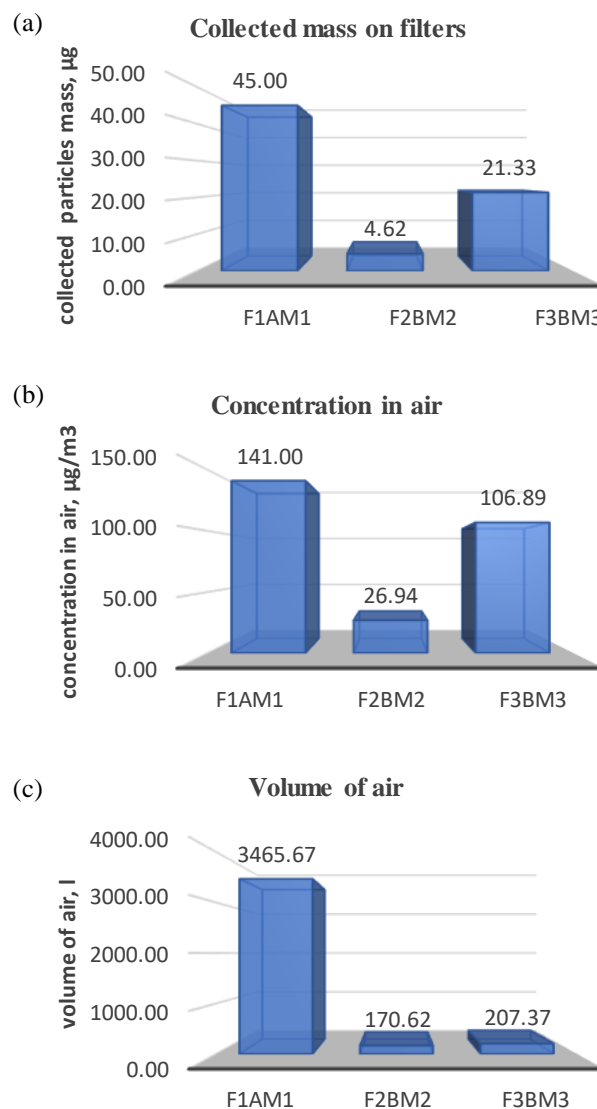


**Fig. 2.** (a) Collected mass on filters; (b) concentration on air; (c) volume of air.



The analysis of the presented data results in a direct correlation between the mass of particles/fibers collected, the concentration of particles in the air, and the volume of air. The highest mass of particles/fibers collected was recorded in the case of FIAM1, at a particle concentration of 141  $\mu\text{g}/\text{m}^3$  and an air volume of 3465 l. In the cases of F2BM2 and F3BM3, the collected mass is lower, either due to the concentration of particles less air in the respective weaving machines, or due to the volume of air sucked by the GilAirPlus pump, also lower.

### Optical microscopy

To identify the fibers collected on filters, the optical microscopy analysis with phase contrast (100x) (Fig. 3a,b) using filter MCE 201 (PP) was performed.

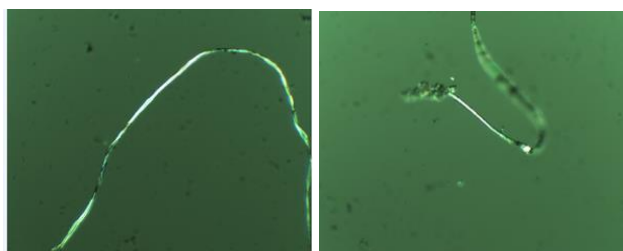


Fig. 3. (a, b) Optical microscopy analysis

Optical microscopy analysis releases the following data:

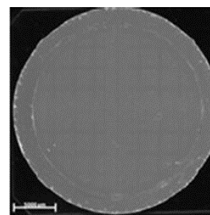
- total number of microscopic fields viewed: 116
- total number of identified fibers: 24;
- fiber diameter between 1-3  $\mu\text{m}$ ;
- fiber length: 3 fibers < 10  $\mu\text{m}$ ; 17 fibers. > 10  $\mu\text{m}$ ;  
4 fibers. > 100  $\mu\text{m}$

### Scanning Electronic Microscopy – SEM

We employ a crossbeam model Auriga produced by Carl Zeiss SMT Germany, and for images, we used the In-Lens detector for secondary electrons located in the column and also local charge compensation CC using nitrogen gas. The images acquired clearly show to us a scattered particle morphology with general nanometric dimensions. The poor contrast is due to charge compensation combined with the non-conductivity of the sample. The acceleration voltage used was 5 kV with a spot size between 2 and 4 (sample current between 0.5 pA and 12pA). The WD distance used is 4.4 mm. In the case of quartz filters, most particles would likely be deposited further inside the filter instead of on the surface, so any microscopical method will not work to determine concentrations. The nucleopore sample has a circular trace with an area of about 336  $\text{mm}^2$  (Fig. 4a). This area was taken into account to be the active area of the filter. For the SEM analysis of sample, five different regions with a surface of 0.46  $\mu\text{m}^2$  were selected on different parts of the sample. The characterized surface is about 0,6% of the entire active area of the filter. High-resolution images a low concentration of particles present on the nucleopore filter (Fig. 4b). The shape and size of the particles were obtained.

Most of the particles have a spherical shape. The statistical data of the apparent size of the measured particles are presented in Table 2.

(a)



(b)

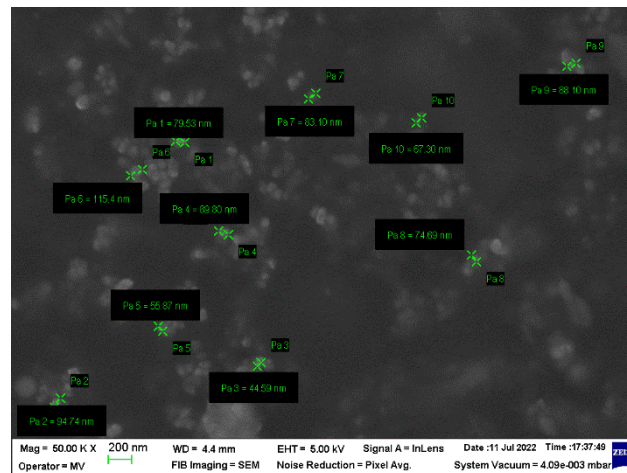


Fig. 4. (a) filter; (b) SEM image

Table 2. Statistical data – PP NMPs size distribution.

N	Valid	30
	Missing	0
Mean	76.3343	
Std. Error of Mean	3.12188	
Median	74.9700 <sup>a</sup>	
Mode	68.32 <sup>b</sup>	
Std. Deviation	17.09922	
Variance	292.383	
Skewness	.400	
Std. Error of Skewness	.427	
Kurtosis	-.262	
Std. Error of Kurtosis	.833	
Range	70.81	
Minimum	44.59	
Maximum	115.40	
Sum	2290.03	
Percentiles	25	63.5000 <sup>c</sup>
	50	74.9700
	75	90.4200

a. Calculated from grouped data.

b. Multiple modes exist. The smallest value is shown

c. Percentiles are calculated from grouped data.

The analysis of the presented data shows the following aspects:

### Variability

The variable has no indicative values. The variable shows the distribution of 50% of the values directed to the left, the median being directed towards the bottom of the box, so the small values are predominant (**Fig. 5b**).

### Distribution form indicators for the analyzed variant

The statistical analysis of the particle sizes showed that 25% have dimensions smaller than 63,5 nm, 25-50% have dimensions between 63,5 nm-74,97 nm, 25% between 74,97 nm-90,42 nm and 25% above 90,42 nm (**Table 2**).

The *asymmetry indices* have the value: of 0.400 which highlights the extent to which the mean deviates from the median and implicitly the curve's normal distribution moves away from the middle, moving to the right.

The *vault indices* have a negative value (-0.262) the curve being of platykurtic type (**Fig. 5a**).

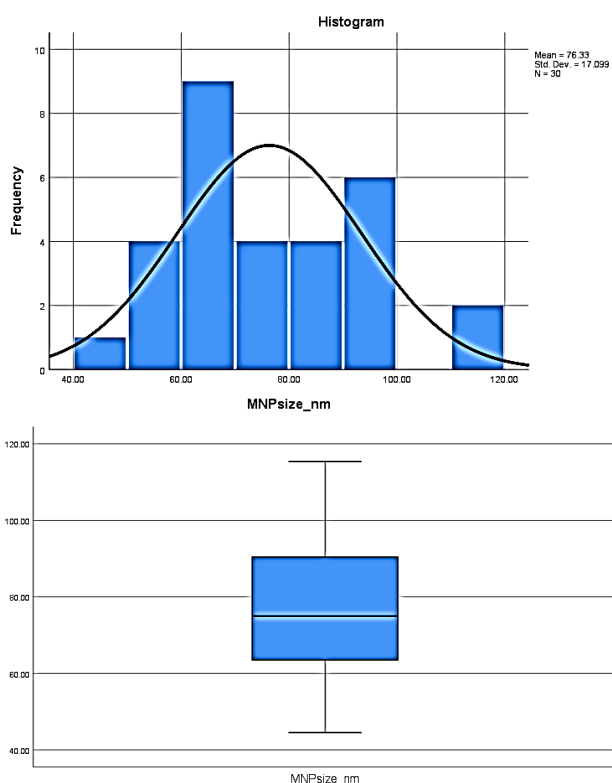


**Fig. 5.** (a) Histogram and (b) Boxplot of the measured particles size.

### Fourier-transform infrared spectroscopy - FTIR

The ATR - FTIR spectra of the PP-SKIM samples were recorded at room temperature using a Perkin-Elmer Spectrum Two IR spectrometer. Attenuated total internal reflection FTIR measurements were performed by averaging 20 scans, with a resolution of 2  $\text{cm}^{-1}$ , over the 4000  $\text{cm}^{-1}$  –500  $\text{cm}^{-1}$  wavenumber range.

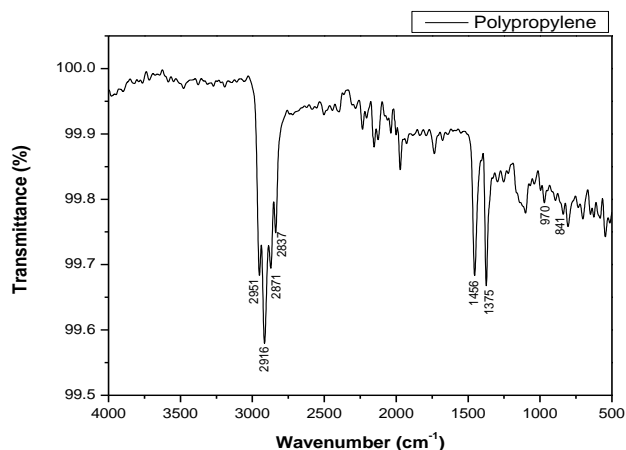


**Fig. 6.** Fourier-transform infrared spectroscopy.

The peaks in the FTIR spectra of the sample are assigned to polypropylene (**Fig. 6**) as follows:

- 2961: asymmetrical stretching  $\text{CH}_3$ ;
- 2916: asymmetrical stretching  $\text{CH}_2$ ;
- 2871: stretching  $\text{CH}_3$ ;
- 1456: symmetrical bending  $\text{CH}_3$ ;
- 1375: symmetrical bending  $\text{CH}_3$ ;
- 970: stretching C-C; 841: rocking C-H.

### $\mu$ -Raman spectroscopy

Unpolarized  $\mu$ -Raman measurements were performed with a triple 557 TriVista spectrometer (S&I Imaging GmbH) in reflection geometry. The excitation was carried out with the 514.5 nm line of DSS laser having an output power level of approximately 100 mW. The laser was focused on the sample with a 100x/0.9 microscope objective to a spot size less than 2  $\mu\text{m}$ . The reflected laser light was rejected by a long-pass edge filter. Raman spectrum was collected with a monochromator having a 1500  $\text{g}/\text{mm}$  grating and a focal length of 750 mm. The spectra acquisition was done with a nitrogen-cooled  $1024 \times 256$  Si-CCD camera. PP particles and fibers were identified using  $\mu$ -Raman spectroscopy. In **Fig. 7** are presented: optical microscope image of microparticles and fibers fraction (a) PP Raman spectra (b) and Raman mapping centered at 1460  $\text{cm}^{-1}$  line of the PP fingerprint.

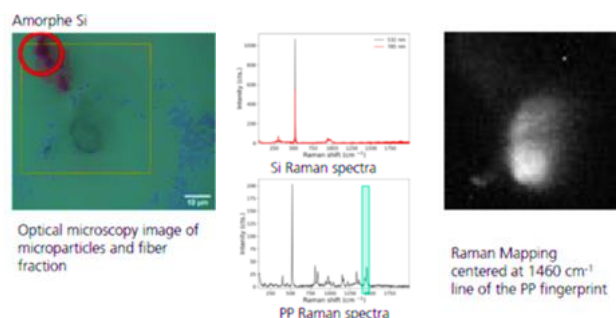


**Fig. 7.**  $\mu$ -RAMAN spectroscopy.

The silica filters with a 9 mm diameter for the collection were used for this is analyze.

### Thermogravimetry and differential scanning calorimetry - TG-DSC

The TG (green) curve is stable, without weight loss but with drift, the mass increased by 105% due to the thermal balance with the vertical system. The DSC (BLUE) curve shows some very small peaks that represent two processes of melting and then decomposition of the PP polymer. (Fig. 8) The quartz erfibers that formed the filter did not undergo any changes and were stable up to 900 °C.

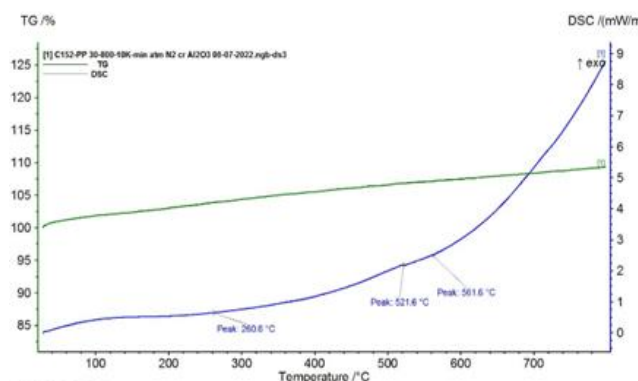


Fig. 8. TG-DSC curves.

## CONCLUSION

In this paper, the results obtained from the registration and collection of polymeric MNPs generated in the technological process of producing narrow fabrics from polypropylene yarns were presented. The collection was made in the vicinity of 3 weaving looms, using 2 types of devices that work at different air flows and 2 types of filters (quartz and gold coated polycarbonate nucleopores), and different amounts of MNPs were obtained on each filter. The highest mass of particles was obtained by using an airflow of 38 l/min on a quartz filter in the vicinity of the M1 machine (average value of the amount collected on the FIAM1 filters of 141  $\mu\text{g}/\text{m}^3$ ); Optical microscopy analyses also confirm the presence of microfibrils collected on quartz fibers. Statistical analysis of the lot size of the collected particles, identified by SEM microscopy indicates an average value of 76.33 nm, while 50% of the values fall in the range 63.5-74.97 nm. From the point of view of the chemical structure, the presence of polypropylene particles from total particles collected on filters is confirmed, by FTIR spectra (peaks specific to molecular bonds in polypropylene polymer),  $\mu$ -RAMAN, and TG-DSC (melting and decomposition point specific to polypropylene). The next challenge is the toxicity tests, which will be performed after collecting biological samples (blood, saliva, nose swap) from the staff that serves these machines.

## ACKNOWLEDGMENTS

This research is carried out within the project: "Understanding exposure and toxicity of Micro- and Nano-Plastic contaminants in humans, POLYRISK" - Horizon 2020, Call: H2020-SC1-BHC-2018-2020" (Better Health and care, economic growth and sustainable health systems) and publishing have been funded by Ministry of Research and Innovation, by Program 1 – Development of the national system for R&D, Subprogram 1.2 – Institutional performance – projects for funding excellence in R&D&I, contract no. 4PFE/30.12.2021.

## CONFLICTS OF INTEREST

There are no conflicts to declare.

## REFERENCES

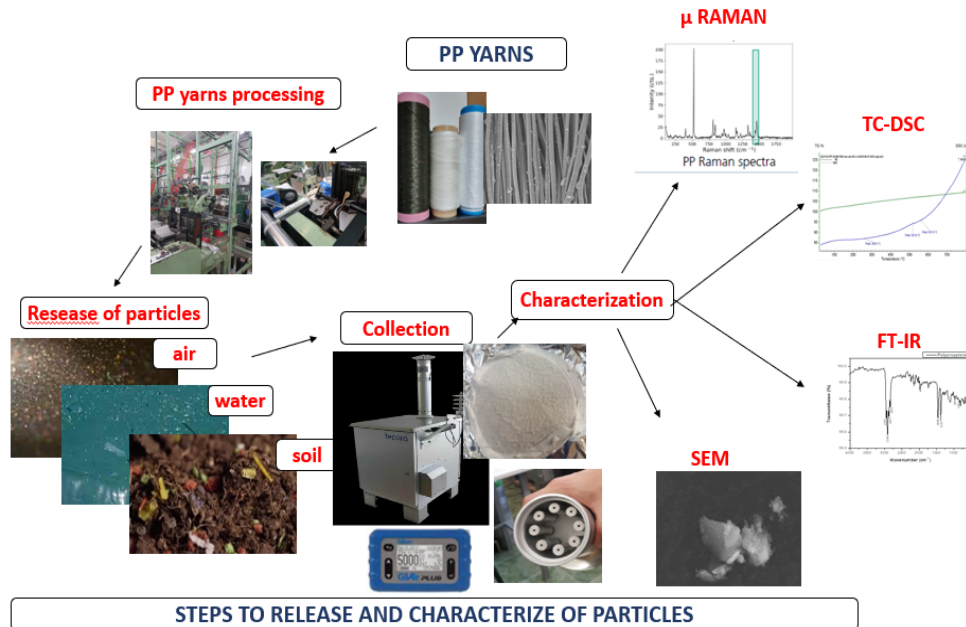
- Adams, J. K.; Dean, B. Y.; Athey, S. N.; Jantunen, L. M.; Bernstein, S.; Stern, G.; Finkelstein, S.A., *Sci. Total Environ.*, **2021**, 784(147155), 1-14.
- Rai, P. K.; Sonne, C.; Brown, R. J.; Younis, S. A.; Kim, K. H.; *J. Hazard. Mater.*, **2022**, 427(127903), 1-22.
- Ugwu, K.; Herrera, A.; Gómez, M.; *Mar. Pollut. Bull.*, **2021**, 169, 112540.
- Klingelhöfer, D.; Braun, M.; Quarcio, D.; Brüggmann, D.; Groneberg, D. A.; *Water Res.*, **2020**, 170, 115358, 1-14.
- Wieland, S.; Balmes, A.; Bender, J.; Kitzinger, J.; Felix Meyer, F.; Ramsperger, A. FRM.; Roeder, F.; Tengelmann, C.; Wimmer, B. H.; Laforsch, C.; Kress, H.; *J. Hazard. Mater.*, **2022**, 428, 128151, 1-20.
- De-la-Torre, G. E.; *J. Food Sci. Technol.*, **2020**, 57, 5, 1601-1608.
- Lin, P.-Y.; Wu, I.-H.; Tsai C.-Y.; Kirankumar R.; Hsieh S.; *Anal. Chim. Acta.*, **2022**, 1198, 339516, 1-7.
- Munyanza J.; Jia Q.; Qaraah, F. A.; Hossain, M. F.; Wu, C.; Zhen, H.; Xiu, G.; *Sci. Total Environ.*, **2022**, **822**, 153339, 1-18.
- Goßmann, I.; Süßmuth, R.; Scholz-Böttcher, B. M.; *Sci. Total Environ.*, **2022**, 832, 155008, 1-9.
- Wang, J.; Li, Y.; Lu, L.; Zheng, M.; Zhang, X.; Tian, H.; Wang, W.; Ru, S.; *Environ. Pollut.*, **2019**, 254 113024.
- Jin, Y.; Wu, S.; Zeng, Z.; Fu, Z.; *Environ. Pollut.*, **2017**, 222, 1-9.
- Prata, J.C.; *Pollut.*, **2018**, 234, 115-126.
- Chen, G.; Feng, Q.; Wang, J.; *Sci. Total Environ.*, **2020**, 703, 135504.
- Paudyal, P.; Semple, S.; Niven, R.; Tavernier, G.; Ayres, J. G.; *Ann. Occup. Hyg.*, **2011**, 55(4), 403-409.
- Sangeetha, B. M.; Rajeswari, M.; Atharsha, S.; Saranyaa Sri, K.; Ramya, S.; *Int. J. Sci. Res.*, **2013**, 3(4), 1-6.
- Tiwari, M.; Babel, S.; *Asian J. Environ. Sci.*, **2013**, 8(1), 64-66.
- Crawford, C.B.; Quinn, B.; *Physicochemical properties and degradation*; Crawford, C.B., & Quinn, B. (Eds.), Elsevier Science, **2017**, pp. 57-100.

## AUTHORS BIOGRAPHY



**Marian-Catalin Grosu** - researcher at The National Research & Development Institute for Textiles and Leather, in the field of textile engineering, was involved in 18 national and international research projects, as coordinator/team member, has more than 40 scientific publications, including 10 Web of Science articles, participated at 20 national and international scientific conferences, innovation exhibitions, and brokerage events, in Romania and abroad, is the co-author of a book, and had a national patent.

GRAPHICAL ABSTRACT



PP is a polymer in the textile industry, it is produced both in the form of fiber and filament, with different fineness (dtex / den). The processing of PP yarns is done by applying classic or unconventional technologies. Mechanical and chemical processes of it leads to the formation of particles releasing into the environment. Determining the concentration of airborne particles and collecting them was done to evaluate the characteristics:  $\mu$ -Raman, TC-DSC, FTIR, SEM.



This article is licensed under a Creative Commons Attribution 4.0 International License, which allows for use, sharing, adaptation, distribution, and reproduction in any medium or format, as long as appropriate credit is given to the original author(s) and the source, a link to the Creative Commons license is provided, and changes are indicated. Unless otherwise indicated in a credit line to the materials, the images or other third-party materials in this article are included in the article's Creative Commons license. If the materials are not covered by the Creative Commons license and your intended use is not permitted by statutory regulation or exceeds the permitted use, you must seek permission from the copyright holder directly.

Visit <http://creativecommons.org/licenses/by/4.0/> to view a copy of this license.